

RESEARCH ARTICLE

Effect of Microwave Hybrid Heating on Mechanical Properties and Microstructure of Sn3.0Ag0.5Cu/Cu Solder Joints

S.R.A. Idris* and M.N. Mazelan¹

Faculty of Mechanical and Automotive Engineering Technology, Universiti Malaysia Pahang Al-Sultan Abdullah, 26600 Pahang, Malaysia

ABSTRACT - Microwave hybrid heating (MHH) has become soldering's alternative method for lead-free solder alloys due to its benefits towards modern microtechnology, such as shorter processing time, lower energy consumption and lower defect rate. Nonetheless, it still requires susceptors to improve its heating performance, such as SiC, which is known for its high loss factor under low microwave frequencies. In this study, the effect of microwave hybrid heating on mechanical properties, as well as the microstructure of solder joint between Sn3.0Ag0.5Cu (SAC305) solder alloy and Cu substrate was investigated. Solder joint was created using MHH with different soldering parameters (amount of SiC in a range of 3-7g and exposure time in a range of 7-10min) between SAC305 solder alloy (in the form of wire and paste) and Cu substrate. Then, a lap shear test was carried out following a standard of ASTM D1002 to determine solder joint strength. Characterization was made using an optical microscope and scanning electron microscopy. Results showed that solder wire produced the highest solder joint strength with the value of 115.45 MPa when using 3.05g of SiC for 8.92min soldering time. Meanwhile, the solder paste produced 109.76MPa solder joint strength when using 3.03 g of SiC for 9.39 min soldering time. The intermetallic compound (IMC) form was scallop-like Cu₆Sn₅, both solder/substrate joints with a thickness of 2.87 μm for solder wire and 3.62 μm for solder paste. Nonetheless, an excessive amount of SiC would generate more heat in MHH and increase the IMC thickness as well as reduce shear strength, which eventually decreases the solder joint stability.

ARTICLE HISTORY

Received : 30th Sept 2022
Revised : 04th Aug 2023
Accepted : 04th Sept 2023
Published : 17th Oct 2023

KEYWORDS

Microwave hybrid heating;
Shear strength;
Intermetallic compound

1.0 INTRODUCTION

Microelectronic systems demanded an increasing urge on the dependability of interconnecting solder joints due to the rapid growth of electronic devices towards volume downsizing and functional integration. In addition, rough working environments such as thermal cycling, vibrations and drop impact make reliable solder joints more crucial [1-3]. Previously, Sn-lead solder was used due to its excellent properties, which include thermal properties and superior wettability. Nonetheless, when Sn-lead solder was prohibited due to its toxicity, several types of Sn-based solders were discovered by other researchers [3-6]. These types of solders possess lower solder joint properties than Sn-lead solder; hence, researchers employed a novel strategy to enhance their properties.

A conventional reflow soldering process is a well-known process that can affect the formation and growth of thin as well as uniform IMC layers. This is important as it represents a good and reliable solder joint strength between solder and substrate material. However, excessive growth of IMC during reflow soldering may lead to poor solder joint strength since IMC is brittle in nature. Previous studies have proved that the use of MHH can be another alternative to create solder joints due to its lower energy usage, high heating rate and less material losses [7-9]. Moreover, heating from a microwave alone is not enough to create a good interconnection between solder and substrate and hence, it needs other sources of heat from external susceptors to make it possible to be considered for soldering. External susceptors include iron powder, silicon carbide and graphite which are being used in the current research [10-12].

Studies have compared SiC with other susceptor materials, such as graphite boats and charcoal, to evaluate its performance in hybrid heating [13]. These comparative analyses provide insights into the advantages and disadvantages of using SiC as a susceptor material. SiC was found to have high energy absorption capabilities during the microwave heating process. This means that it can efficiently convert microwave energy into heat, making it a suitable material for heating applications. SiC can also be used as a microwave susceptor due to its high loss factor under low microwave frequencies [14]. Overall, studying SiC in microwave hybrid heating allows researchers to optimize energy absorption, heating rates, and temperature capabilities, leading to more efficient and effective heating processes in various applications. Even though those studies suggested that SiC can be used as a susceptor material in microwave hybrid heating, its amount and content can affect the formation of IMCs, which is still not properly addressed. Hence, in this study, the research is focused mainly on exploring microwave hybrid heating to produce high solder joint strength as well as the transformation of IMC layer, especially for powder compacted solder in comparison with wired solder type.

*CORRESPONDING AUTHOR | SRA. Idris | ✉ rabiattull@ump.edu.my

2.0 EXPERIMENTAL SETUP

2.1 Sample Preparation

In the study, a substrate, which is a pure copper rod of 10 mm length×6 mm diameter and a copper plate of 10 mm×10 mm×2 mm were prepared, ground, and cleaned ultrasonically to ensure there are no impurities attached to the surface of the substrate. Solder wires were coiled to 6 mm diameter for ease of soldering and then were cleaned in an ultrasonic cleaner.

2.2 Soldering Procedure

Soldering between SAC305 solder alloy (both wire and paste type) and Cu substrate was conducted in a microwave oven (Panasonic NN CD997S, 1000 W, 2.45 GHz), as shown in Figure 1. No clean flux was applied to the surface of the substrate in order to clean it from contamination as well as to ensure the solderability between the solder and substrate. The solder was then sandwiched between the substrate and made ready for soldering. The parameters used for soldering is stated in Table 1. After the soldering, the specimen was removed from the microwave and cooled in air.

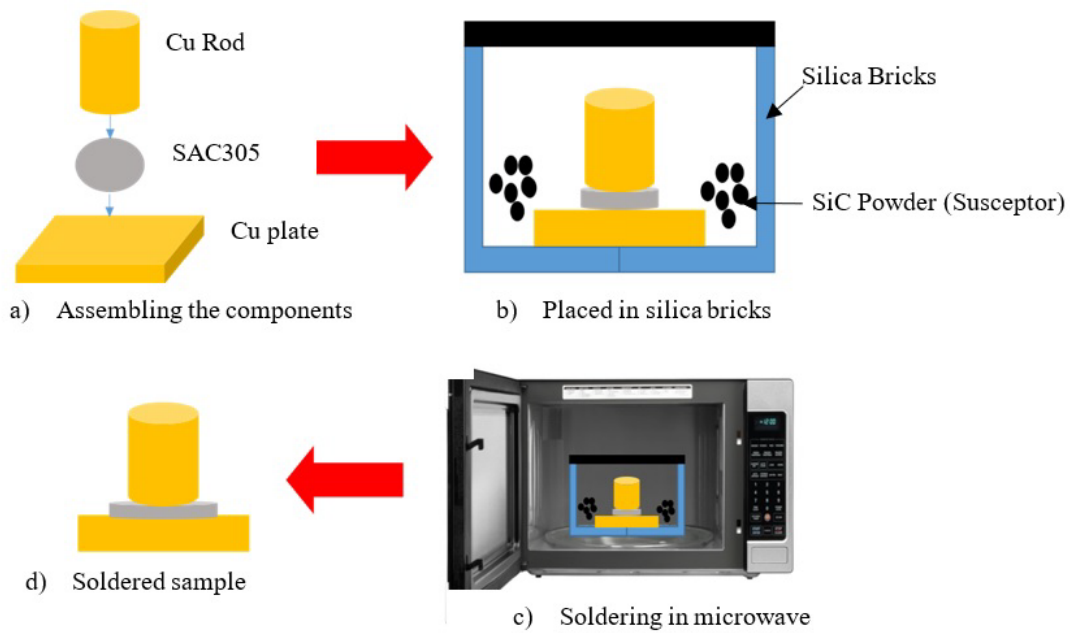


Figure 1. Schematic diagram of the soldering process step

Table 1. Optimization goal for the variables and response

Name	Goal
Exposure time (minutes)	In range (7 to 10)
Amount of susceptor (g)	In range (3 to 7)
Shear strength	Maximized

2.3 Lap Shear Test Preparation

The shear strength of IMC was analyzed by conducting the lap shear test. The lap shear test is frequently used to examine the strength of the adhesive and/or interface strength bonded with adhesives. In this study, the lap shear test was conducted following the ASTM D1002 standard. The crosshead speed was set to 1 mm/min, and the test was performed in a standard laboratory atmosphere. For every set of parameters, four specimens were taken for the lap shear test, and the average value was calculated. Figure 2 displays the setup for the shear test.

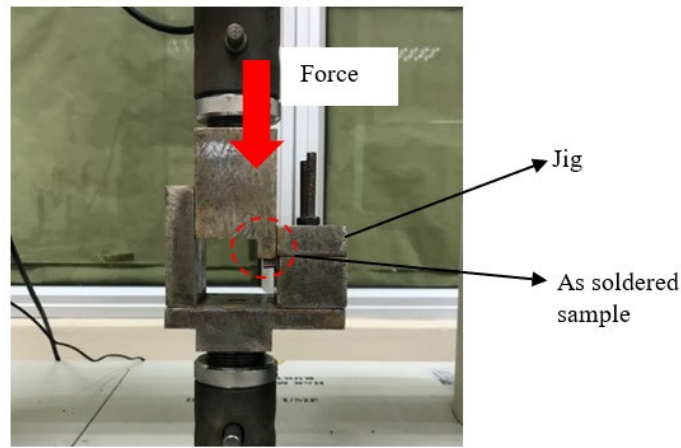


Figure 2. Experimental setup for shear test

2.4 Characterization Methods

The cross-sectional images of the solder joints were observed with optical microscopy and scanning electron microscopy – energy dispersive x-ray (SEM-EDX). The specimen was immersed in an acid solution of 5 ml hydrochloric acid and 95 ml ethanol for several minutes to remove the solder by etching completely. Then, they were characterized in terms of IMC type and thickness.

3.0 RESULTS AND DISCUSSION

3.1 Shear Strength of SAC305/Cu Solder Joints

Since solder joints are frequently subjected to mechanical loading throughout their service lives, their mechanical properties, such as shear strength, have a major effect on the reliability of overall electronic packaging. Therefore, a series of shear strength tests were conducted for both solder types (wire and paste) of SAC305/Cu joints to determine their shear strength. Average values of shear strength for the SAC305 wire/Cu joint and SAC305 paste/Cu joint sample are presented in Table 2 and Table 3, respectively. The test was conducted three times for each sample. For wire SAC305/Cu joints, sample 1 has the lowest shear strength value of 60.51 MPa. It was produced by 4g of susceptor for 7 minutes. The joint produced by 6g of susceptor for 9 minutes resulted in the highest shear strength (sample 4). Sample 3 showed the second-highest shear strength (96.74 MPa) with only a 1.0 MPa difference from sample 4. Samples 9 to 13 showed approximately the same results of shear strength ranging from 87.32 MPa to 95.85 MPa.

On the other hand, in SAC305 solder paste/Cu joints, it was observed that sample 7 has the highest shear strength value (107.38MPa) as it has been produced with 8 minutes exposure time and 3 g susceptor. The second highest shear strength of 106.53 MPa was achieved with 5 g of susceptor for 6 minutes (sample 5). Sample 4 has the lowest shear strength with a value of 86.32 MPa. Samples 9 through 13 have the same parameters (5 g susceptor and 8 minutes exposure time), and the shear strength ranged from 96.35 MPa to 92.23 MPa. Figure 3 summarizes the shear strength for wire solder and solder paste in Table 2 and Table 3. These shear strength results showed improvement compared to the previous study, where the highest shear strength value was 57.5MPa after reflow soldering with 5 s of ultrasonic treatment [15].

Table 2. Shear strength result according to the experiment order for SAC305 wire

Sample	Amount of susceptor (g)	Exposure time (minutes)	Shear strength (MPa)
1	4	7	60.51
2	4	9	88.44
3	6	7	96.74
4	6	9	97.38
5	5	6	80.47
6	5	10	90.17
7	3	8	64.91
8	7	8	92.65
9	5	8	89.94
10	5	8	95.85
11	5	8	87.32
12	5	8	93.32
13	5	8	93.71

In general, solder paste produced better solder joint strength even with a small amount of susceptor and shorter exposure time. This was expected since solder paste can easily melt and diffuse into Cu substrate to form strong as well

as reliable IMC. The chemical reaction in the bulk solder paste makes it easier to react. Meanwhile, solder wire requires more time to melt and react with Cu substrate; hence producing lower solder joint strength.

Table 3. Shear strength result according to the experiment order for SAC305 paste

Sample	Amount of susceptor (g)	Exposure time (minutes)	Shear strength (MPa)
1	4	7	103.89
2	4	9	94.12
3	6	7	94.85
4	6	9	86.32
5	5	6	106.53
6	5	10	96.12
7	3	8	107.38
8	7	8	91.09
9	5	8	93.36
10	5	8	93.03
11	5	8	93.69
12	5	8	92.23
13	5	8	96.35

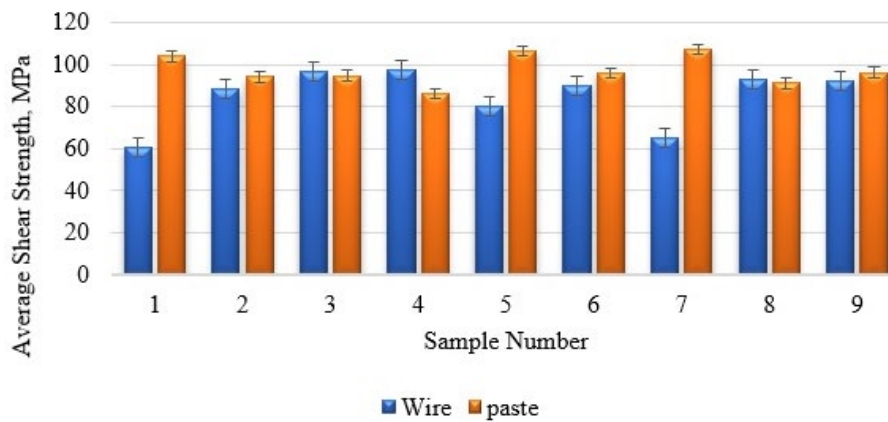


Figure 3. Comparison of shear strength for both forms of SAC305 according to the experiment order

The fracture mechanism of the solder joints was investigated by examining the fracture surfaces of the solder joints. Figure 4 displays the shear fracture surface for solder wire (a) and solder paste (b). Based on the figures, fracture surface smearing can be seen, which is a common phenomenon as the loading direction is parallel to the fracture surface. The presence of this dimple-like elongated structure suggests that it is a ductile fracture mode that had occurred in the solder area (failure mode I). The same finding was found in a previous research [16]. Ductile failure is a mode of fracture that occurs following considerable plastic deformation. During ductile failure, a part will experience a localized reduction in area due to plastic deformation until it ultimately fractures. The fracture appearance is rough and torn, and the cross-section is reduced or distorted. Shear lips are observed at the latter part of the fracture and indicate the final failure of the part. The fracture surface is dull, with a fibrous appearance. These results proposed that the IMC layer is stronger than the solder matrix. Both shear fractures occurred at the bulk solder.

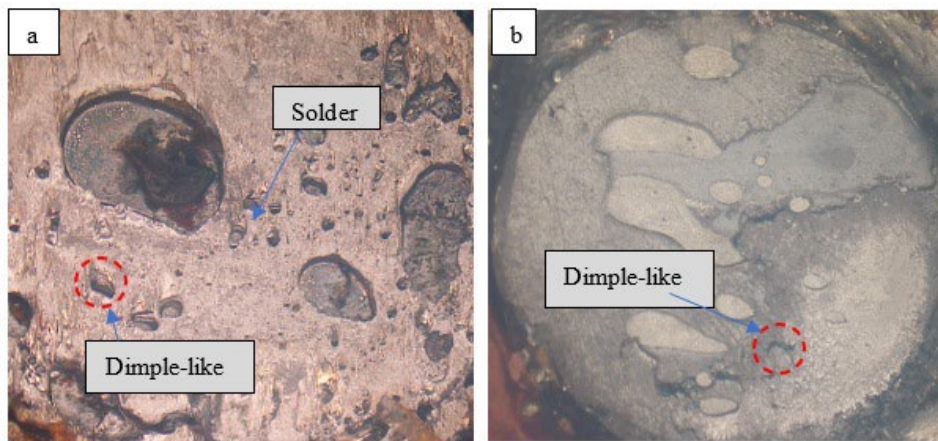


Figure 4. Shear fracture surface for (a) solder wire and (b) solder paste

In addition, the effect of experiment parameters on the shear strength was also recorded. According to the results, interactions between the factors did not record a significant p-value at a 95% confidence level in both forms of solder. However, the interaction plot showed that there is an interaction occurred between exposure time (A) and the amount of susceptor (B). Figure 5(a) and 5(b) display the interaction plot for both solder wire and solder paste, respectively, obtained from the design expert software. Based on Figure 5 (a), the amount of susceptor (B) shows a significant effect on shear strength compared to exposure time (A). As the amount of susceptor increases, the shear strength also increases. Different interaction was observed for solder paste. From Figure 5 (b), it was observed that a low amount of susceptor and exposure time will result in higher shear strength. Two different interactions observed between solder wire and solder paste imply that these two forms of solder possess different microstructures.

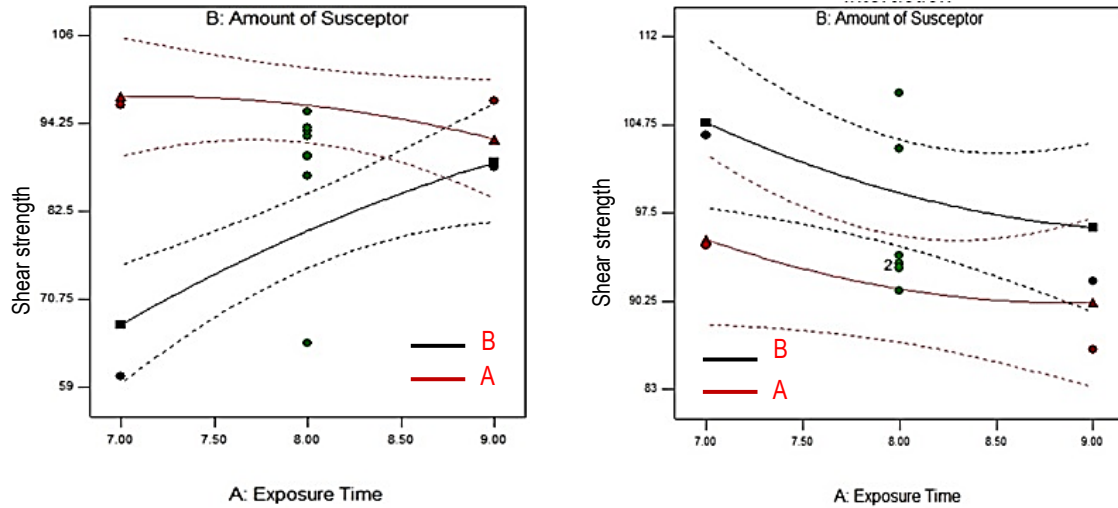


Figure 5. Interaction plot for (a) solder wire and (b) solder paste

3.2 Intermetallic Compound Formation at SAC305/Cu Solder Joint

The optimized soldered sample that yielded the highest shear strength was selected to analyze the microstructure and its IMC thickness. Figure 6 and Figure 8 show the cross-section image of the optimized sample for wire solder form and paste shear form, respectively, with the highest shear strength (3.05 g SiC, 8.92 minutes and 3.03 g SiC, 9.39 minutes). Meanwhile, Figure 7 and Figure 9 show an EDX analysis from the top view, confirming the IMC type formed after soldering. As seen in Figure 6, a scallop shape Cu_6Sn_5 was observed at the solder/substrate interface as well as spallation. The gap between the neighboring scallops was far, which may be due to the coarsening of scallop Cu_6Sn_5 . According to a previous study, this reaction is governed by the Gibbs-Thomson effect in the ripening process [17]. Smaller IMC grains were dissolved in the liquid solder, making the growth of neighboring grains elevated. Other than Cu_6Sn_5 , Cu_3Sn was also observed at the SAC/Cu interface. Precipitation of Cu_3Sn becomes thermodynamically possible after the precipitation of Cu_6Sn_5 [17]. The Cu_3Sn is said to be grown by solid-state diffusion while scallop shape Cu_6Sn_5 by the ripening process.

For the solder paste in Figure 8, it can be seen that the IMC observed at the solder/substrate interface were Cu_6Sn_5 and Cu_3Sn . Scallop-like and polygon-like (sharp edges) IMC peaks were observed. The IMC shape and size were different from each other. It signifies that they have different growth stages due to the different IMC distributions on the Cu substrate. The IMC shape was mostly polygon-like. It may be due to the incomplete ripening process. Spallation was observed, as well as a far gap between the adjacent scallops. The spalling of Cu_6Sn_5 was observed because the Sn concentration in SAC305 was high. The evolution of IMCs at the SAC/Cu solder joint is based on the continuous growth of Cu_6Sn_5 (from soldering) and the formation of Cu_3Sn . The formation of Cu_3Sn from Cu_6Sn_5 is shown as follows:



Alternatively, Cu_3Sn could dissolve itself and react with the Sn atom to produce Cu_6Sn_5 . The formation of Cu_6Sn_5 is governed by the following transformation equation:



Figure 10 presents the average IMC thickness of the optimized soldered sample (wire and paste) which has the highest shear strength. Based on the table, the average IMC thickness for both solder form is less than $4 \mu m$, which are considered thin for first-level packaging. The standard deviation for wire solder form is 0.76, while for solder paste is 1.73, which is considered quite high. This result is in relation to the cross-section image. Based on Figure 6, the scallop-like IMCs were close together, and the adjacent scallop was close together. This results in a standard deviation of less than 1. The same concept applies to the solder paste. Figure 8 shows that the IMCs have sharp edges, and the adjacent scallops are far apart,

resulting in a standard deviation of more than 1. Meanwhile, Figure 11 shows XRD results, which confirm the existing compound was Cu_3Sn and Cu_6Sn_5 IMC for both solder wire and solder paste.

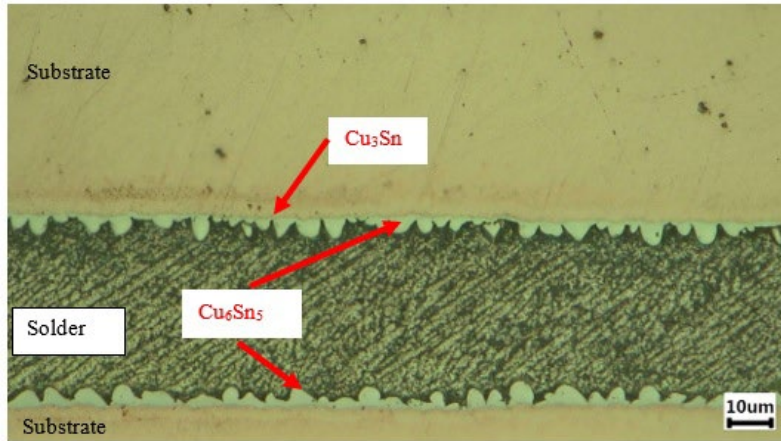
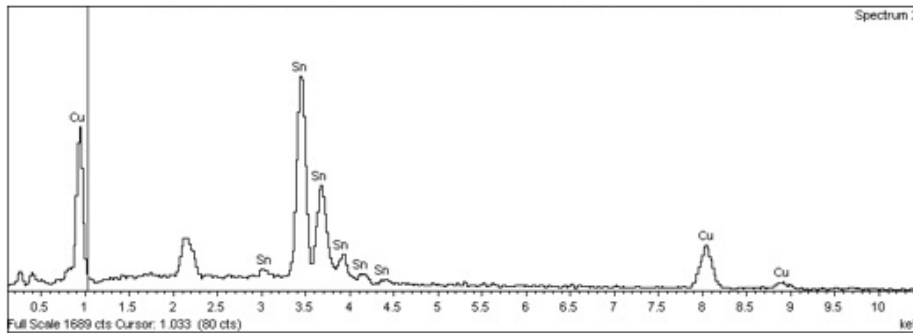
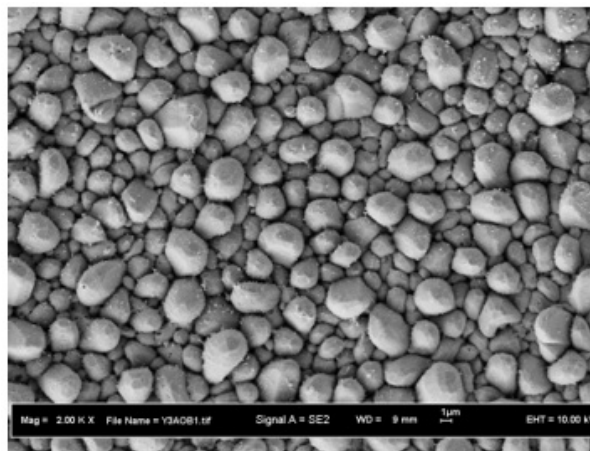


Figure 6. Cross section of an optimized soldered sample of Sn-Ag-Cu (wire)/Cu from sample 3



Element	App Conc.	Intensity Corr	Weight%	Weight% Sigma	Atomic%
Cu L	9.61	0.4394	38.52	0.90	53.92
Sn L	32.52	0.9312	61.48	0.90	46.08
Totals			100.00		

Figure 7. EDX results of interface intermetallic formed at Sn-Ag-Cu (wire)/Cu solder joint from sample 3

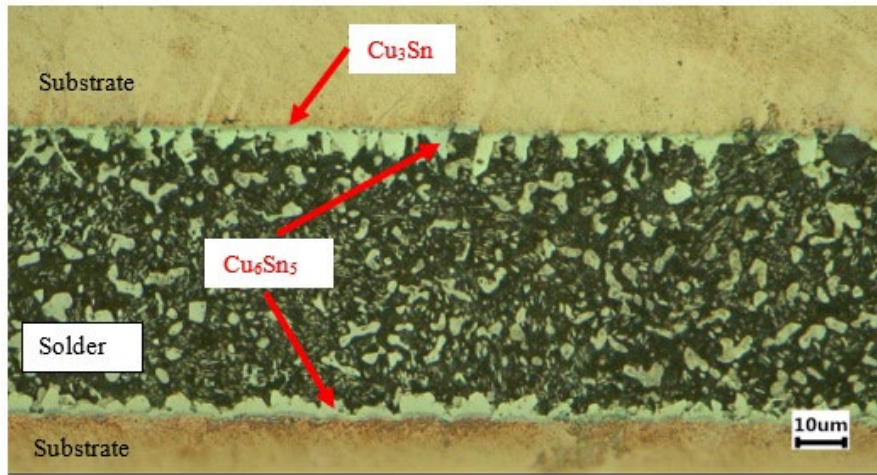
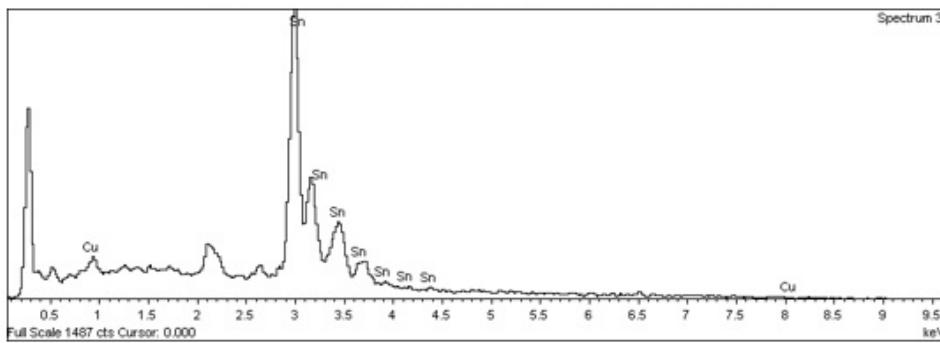
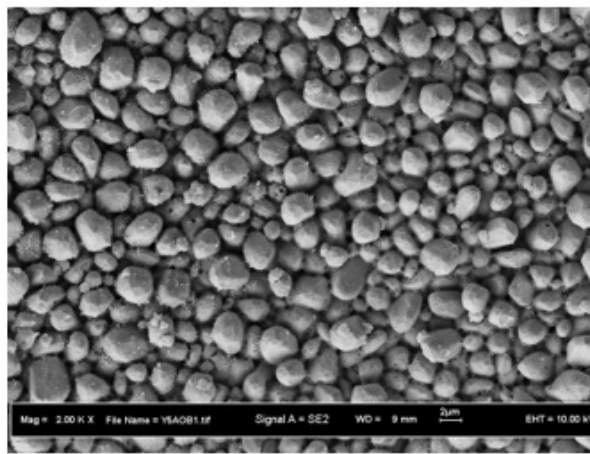


Figure 8. Cross section of an optimized soldered sample of Sn-Ag-Cu (paste)/Cu from sample 2



Element	App Conc.	Intensity <u>Comp</u>	Weight%	Weight% Sigma	Atomic%
Cu L	0.13	0.5054	11.43	2.85	19.43
Sn L	1.93	0.9775	88.57	2.85	80.57
Totals			100.00		

Figure 9. EDX results of interface intermetallic formed at Sn-Ag-Cu (paste)/Cu solder joint from sample 2

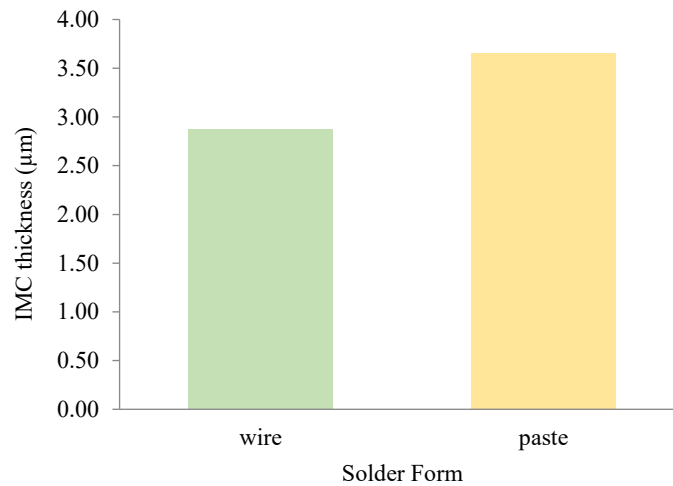


Figure 10. Average IMC thickness for optimized solder wire and solder paste

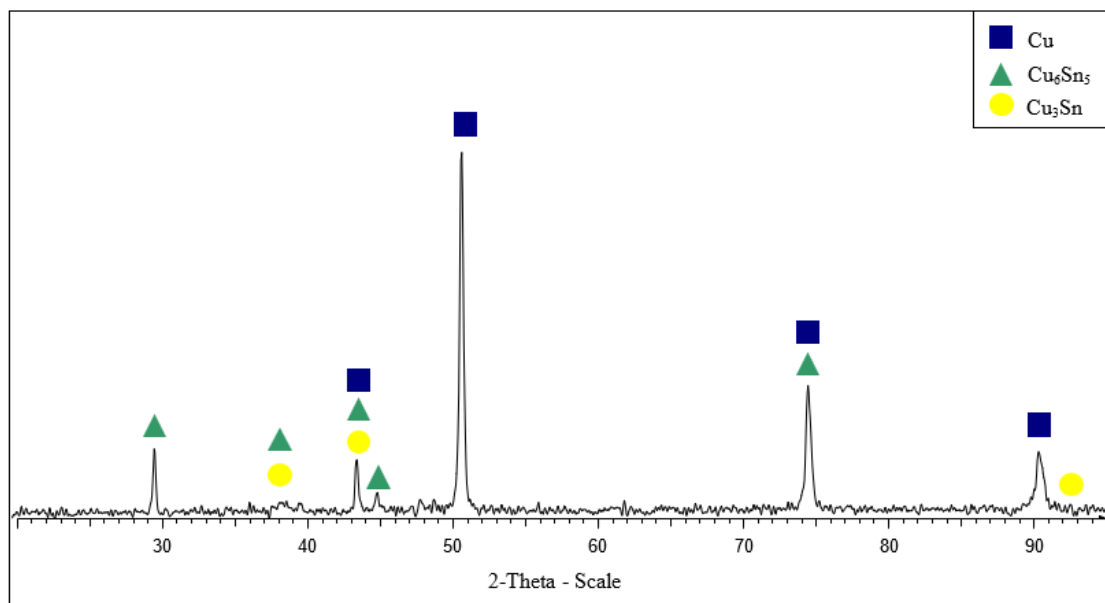


Figure 11. XRD spectrum of Sn-Ag-Cu/Cu solder joint

4.0 CONCLUSIONS

In this study, the effect of microwave hybrid heating on mechanical properties as well as the microstructure of solder joint between Sn3.0Ag0.5Cu (SAC305) solder alloy and Cu substrate, was investigated. The results concluded that:

- i. Solder wire produced the highest solder joint strength with a value of 115.45 MPa when using 3.05 g of SiC for 8.92 minutes of soldering time. Meanwhile, the solder paste produced 109.76 MPa solder joint strength when using 3.03 g of SiC for 9.39 minutes of soldering time.
- ii. The intermetallic compound (IMC) form was scallop-like Cu_6Sn_5 , both solder/substrate joints with a thickness of 2.87 μm for solder wire and 3.62 μm for solder paste. Nonetheless, an excessive amount of SiC would generate more heat in MHH and increase the IMC thickness as well as reduce shear strength, which eventually decreases the solder joint stability.

5.0 ACKNOWLEDGEMENT

The authors would like to thank for the financial support for this work from FRGS/1/2018/TK03/UMP/02/21 (RDU190152) by the Ministry of Higher Education for providing the research facilities.

6.0 REFERENCES

- [1] K. Choi, D. Y. Yu, S. Ahn, K. H. Kim, J. H. Bang, and Y. H. Ko, "Joint reliability of various Pb-free solders under harsh vibration conditions for automotive electronics," *Microelectronics Reliability*, vol. 86, pp. 66-71, 2018.

- [2] Y. Xiao, Q. Wang, L. Wang, X. Zeng, M. Li, *et al.*, "Ultrasonic soldering of Cu alloy using Ni-foam/Sn composite interlayer," *Ultrasonics Sonochemistry*, vol. 45, pp. 223-230, 2018.
- [3] C. J. Lee, K. D. Min, H. J. Park, and S. B. Jung, "Mechanical properties of Sn-58 wt%Bi solder containing Ag-decorated MWCNT with thermal aging tests," *Journal of Alloys and Compounds*, vol. 820, pp. 153077, 2020.
- [4] Q. Lin, C. Ye, and R. Sui, "Wetting of Ni-based amorphous and crystalline alloys by Sn and Sn-based solders," *Microelectronics Reliability*, vol. 111, p. 113722, 2020.
- [5] T. T. Kyaw, P. Tunthawiroon, K. Kanlayasiri, K. Yamanaka, and A. Chiba, "A study on wettability and formation of intermetallic phase between Co-Cr-Mo alloy and Sn-Solder used as a potential under bump metallization for flip-chip packages," *Intermetallics*, vol. 125, pp. 106875, 2020.
- [6] L. Yin, Z. Zhang, Z. Su, H. Zhang, C. Zuo, *et al.*, "Interfacial microstructure evolution and properties of Sn-0.3Ag-0.7Cu-xSiC solder joints," *Materials Science and Engineering A*, vol. 809, pp. 140995?, 2021.
- [7] A. Upadhyaya, S. K. Tiwari, and P. Mishra, "Microwave sintering of W-Ni-Fe alloy," *Scripta Materialia*, vol. 56, pp. 5-8, 2007.
- [8] T. L. Alford, M. J. Gadre, R. N. P. Vemuri, and N. D. Theodore, "Susceptor-assisted microwave annealing for activation of arsenic dopants in silicon," *Thin Solid Films*, vol. 520, pp. 4314-4320, 2012.
- [9] M. A. A. Mohd Salleh, S. D. McDonald, Y. Terada, H. Yasuda, and K. Nogita, "Development of a microwave sintered TiO₂ reinforced Sn-0.7wt%Cu-0.05wt%Ni alloy," *Materials & Design*, vol. 82, pp. 136-147, 2015.
- [10] M. Lutfi, F. Yusof, S. Ramesh, T. Ariga, and M. Hamdi, "Effect of microwave hybrid heating on the formation of intermetallic compound of Sn-Ag-Cu Solder Joints," *Electronics Manufacturing Technology Conference (IEMT)*, vol. 36, pp. 1-5, 2014.
- [11] S. Mohamad Faizal and O. Saliza Azlina, "Intermetallic compound formation on lead-free solders by using microwave energy," in *AIP Conference Proceedings*, 2016, pp. 060008.
- [12] N. M. Maliessa and S. R. A. Idris, "Effect of different amount of silicon carbide on SAC solder-Cu joint performance by using microwave hybrid heating method," in *IOP Conference Series: Materials Science and Engineering*, 2019, pp. 012110.
- [13] N. K. Bhoi, H. Singh, and S. Pratap, "A study on microwave susceptor material for hybrid heating," *Journal of Physics: Conference Series*, vol. 1240, p. 012097, 2019.
- [14] H. Lun, Y. Zeng, X. Xiong, L. Zhao, D. Li, *et al.*, "The effect of sic content on microstructure and microwave heating rate of h-BN/SiC ceramics fabricated by spark plasma sintering," *Materials*, vol. 12, p. 1909, 2019.
- [15] X. Hu, H. Xu, W. Chen, and X. Jiang, "Effects of ultrasonic treatment on mechanical properties and microstructure evolution of the Cu/SAC305 solder joints," *Journal of Manufacturing Processes*, vol. 64, pp. 648-654, 2021.
- [16] J. Jing, F. Gao, J. Johnson, F. Z. Liang, R. L. Williams, and J. Qu, "Brittle versus ductile failure of a lead-free single solder joint specimen under intermediate strain rate," *IEEE Transactions on Components, Packaging and Manufacturing Technology*, vol. 1, pp. 1456-1464, 2011.
- [17] L. M. Lee and A. A. Mohamad, "Interfacial reaction of Sn-Ag-Cu lead-free solder alloy on Cu: A review," *Advances in Materials Science and Engineering*, vol. 2013, p. 123697, 2013.